Chapter 1

Introduction

1.1 Background

Matter and charge transport properties of oxides are of profound importance for a number of oxide characteristics. Depending on application and desired properties, the transport rates should be either high or low. In both cases it is of scientific as well as technological importance to understand the underlying chemical and physical principles and to find means of controlling the transport properties.

Knowledge of conditions for the growth of adherent metal oxides with low densities of pores and other macroscopic defects is essential for optimal protection of high-temperature materials in service. When oxide growth takes place predominantly at the oxide-gas interface, for example on Cr, poor adherence of the scale is often observed [1]. In systems where oxides growth takes place predominantly at the substrate-oxide interface, cracks can often be found in the oxide scale. An effective way to repair an oxide containing pores, voids and cracks is to fill these with new "material".

This material is comprised basically of metal and oxygen, which implies the need for transport of both oxygen (ions) and metal (ions) to these positions. To realize this, one needs to be able to vary the position of oxide growth in the metal-oxide system of interest.

The beneficial influence on the oxidation behavior of high temperature materials by the addition of rare earth metals (REM) such as Y, Hf, Ce and La is a well-known phenomenon [2-6]. The reactive element effect manifests itself giving a good resistance to spallation at high temperature and during cooling down to room temperature [7-8]. Several mechanisms have been proposed to explain these REM effects [9-14]. There are similar positive effects by the addition of certain noble metals such as Pt [15]. However, the mechanisms behind the effects of all these additions are not clearly identified and several possible mechanisms have been discussed for a long time [16-18].

Transport of gases in oxides can take place in molecular, atomic and ionic form. It is important to identify these different diffusing species of gases in oxides in order to control various processes, such as formation of good-quality oxides on semiconductors and to control oxidation of metallic materials [19-22]. Another important field concerns oxygen transport in yttria stabilized zirconia (YSZ), which is probably the most widely used material in solid oxide fuel cells (SOFC) at high temperatures, but it is also used in oxygen separators, pumps and membranes because of its high ionic conductivity. To be able to improve the efficiency at low temperatures, enhancement of the ionic conductivity

of YSZ is necessary. At the same time, the non-ionic (molecular and atomic) oxygen passing between the anode and cathode should be minimized because the diffusion of molecules and atoms through the electrolyte can lower the efficiency of the fuel cells. Numerous studies have been carried out on oxygen transport in yttria stabilized zirconia. However, most of them only deal with the ionic conductivity at high temperatures by using impedance spectroscopy, which exclusively measures the charge transfer. Then an important question is how to separate the contributions of molecules, atoms and ions to the overall transport of diatomic gases in oxides.

An analysis of literature data of permeability of monatomic gases (He, Ne, Ar and Kr) and diatomic gases (hydrogen, oxygen and nitrogen) in vitreous silica at 900°C indicates the diffusion of hydrogen, oxygen and nitrogen in the material does not only take place in molecular form. Lee *et al* investigated the diffusion of hydrogen in silica and observed two diffusion regimes, called "normal" and "abnormal diffusion". To find out the reasons for these observations is of scientific importance.

1.2 Aims of this work

The overall aim of the thesis work has been to contribute to understanding of the fundamental mechanisms of transport in oxides, especially, the transport mechanisms of the diatomic gases hydrogen, oxygen, and nitrogen in vitreous silica and zirconia. The following aspects are addressed.

- An experimental method to identify transporting species of gases and their contributions to the overall transport in oxides is developed and exemplified in Papers 3 and 8.
- Paper 4 presents a novel and relatively straightforward method to quantify diffusion and amount of gas present in oxide scales.
- The effects of platinum on the oxidation of metals are investigated with the use of gas phase analysis and the ^{18}O-SIMS technique in Papers 1 and 6.
- Transports of diatomic gases in vitreous silica are studied in Papers 2 and 3.
- Transports of gases in yttria-stabilized zirconia are investigated in Papers 7 and 8.

References

1. B. Tveten, G. Hultquist, and T. Norby, Oxid. Met., 51 (1999), 221
2. F. A. Golightly, F. H. Stott, and G. C. Wood, Oxid. Met., 10 (1976), 163
3. D. P. Whittle and J. Stringer, Phil. Trans. R. Soc. London A, 295 (1980), 309
4. J. Stringer, Mater. Sci. Eng. A, 120 (1989), 129
5. P. Hou, V. Chia and I. Brown, Surf. Coatings Technol., 51 (1992), 73
6. R. J. Hussey and M. J. Graham, Oxid. Met., 45 (1996), 349

7. C. H. Xu, W. Gao, and S. Li. Corros. Sci., 43 (2001), 671
8. A. Bautista, F. Velasco, and J. Abenojar. Corros. Sci., 45 (2003), 1343
9. F. H. Stott, G. C. Wood, and F. A. Golightly, Corros. Sci., 19 (1979), 869
10. J. R. Nicholls and P. Hancock, Role of Active Elements in the Oxidation Behaviour of High-Temperature Metals and Alloys, E. Lang ed., Elsevier, London, 1989
11. C. M. Cotell, G. J. Yurek, R. J. Hussey, D. F. Mitchell, and M. J.Graham, Oxid. Met., 34 (1990), 173
12. A. Strawbridge and R. A. Rapp, J. Electrochem. Soc., 144 (1994), 1905
13. B. A. Pint, Oxid. Met., 45 (1996), 1
14. H. Liu, M. M. Stack, and S. B. Lyon, Solid State Ionics, 109 (1998), 247
15. E. J. Felton, Oxid. Met., 10 (1976), 23
16. D. L. Douglass, P. Kofstad, A. Rahmel and G. C. Wood, Oxid.Met., 45 (1996), 529
17. J. Jedlinki. Solid State Phenomena, 21-22 (1992), 335
18. B. A. Pint, Oxid. Met., 48 (1997), 303
19. G. Hultquist, B. Tveten, E. Hörnlund, M. Limbäck, and R. Haugsrud, Oxid. Met., 56 (2001), 313
20. G. Hultquist, B. Tveten, and E. Hörnlund, Oxid. Met., 54 (2000), 1
21. W. J. Quadakkers, P. Schaaf, N. Zhang, A. Gil, E. Wallura, Mater. Corros., 48 (1997), 28
22. W. Beallfower and A. H. Edwards, J. Non-Cryst. Solids, 222 (1997), 33

Chapter 2

Transport in oxides

Diffusion is one of the most important phenomena in solids because it influences many material applications [1, 2]. For example, the corrosion resistance of metallic materials in chemically aggressive environments is improved by forming protective oxide films on the surface of substrates via diffusion-controlled processes. The lifetime of the common electric lamp bulbs is ultimately determined by the permeability of oxygen from the surrounding atmosphere in the gas envelope. The efficiency of full cells at low temperature can be improved by minimizing the non-ionic oxygen to pass over the electrolyte. Depending on applications, the diffusion should be either high or low.

2.1 Transport of gases in oxides

2.1.1 Physical diffusion and diffusion with chemical reactions

- Physical diffusion

The term "physical diffusion" refers to the diffusion of species without chemical interaction with the material. Examples of such diffusion include the diffusion of inert gases (helium, neon, argon, krypton, and xenon), and the diffusion of chemically reactive gases such as hydrogen and oxygen in dielectrics at sufficiently low temperatures ruled by the diffusion rate.

There are several technical terms often used in the study of diffusion: diffusivity, solubility, and permeability. The diffusivity (D), or diffusion coefficient, refers to the rate of movement of individual species, which determines the time necessary to reach steady state flux. The solubility (S) refers to the dissolved gas concentration per unit of applied pressure of gas under consideration. The permeability (P) is the flux through a membrane at steady state, which is the product of the diffusivity and the solubility of the gas in the material of interest. These parameters are related through the expression,

$$P = D\,S \tag{2.1}$$

Obviously, the determination of any two of these parameters automatically defines the value of the third one.

Flux techniques require the formation of a membrane of the materials to be studied. The membrane is heated to a desired measurement temperature, and the gas to be studied is applied at a known pressure to one side of the membrane. Flux of gas through the membrane is monitored as a function of time until the flux becomes time-independent, which indicates that steady state flux occurs. After the steady state flux is obtained, the gas is rapidly removed from the gas-supply side of the membrane and the rate of gas release into the detector system is recorded until no decreases can be seen, which is normally a few percent of the steady state flux value. A typical curve for the flux versus time is shown in Fig. 2.1.

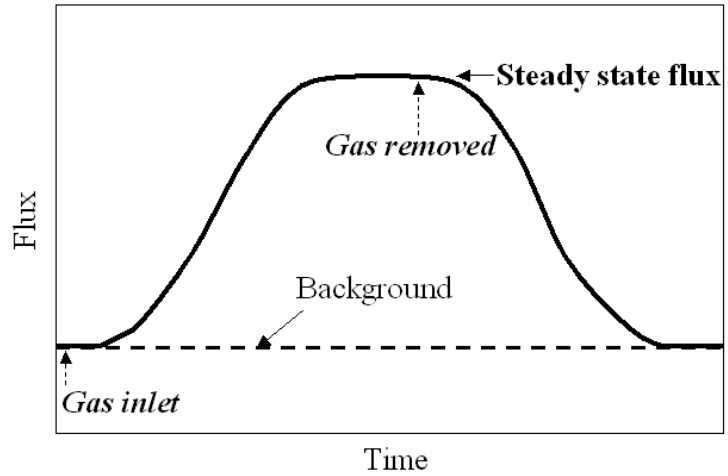

Fig. 2.1 Flux measurement during gas permeation through a membrane.

The diffusivity can be determined from either the rate of rise to steady state flux or from the rate of decay of the flux after removal of the gas from the gas supply side of the membrane [3].

Determination of gas solubility in materials is obtained from the uptake/release method, which is usually measured by either pressure changes in a system of known volume [4] or mass changes using a microbalance [5]. The actual dissolved gas concentration can be measured by infrared or Raman spectroscopy in some cases.

The determination of permeability is based on the flux at steady state measured by using a mass spectrometer tuned for the gas of interest [1]. The permeating gas is continuously removed from the detector system by a vacuum pump. The permeability can be calculated by the following expression,

$$P = F L / A p \qquad (2.2)$$

where F is the flux at steady state, L and A are the thickness and area of the membrane, and p is the pressure of applied gas.

- Diffusion with chemical reactions

Many processes in materials are controlled by the diffusion of reactive molecules either to reaction sites or away from decomposition sites. The more commonly studied process involves hydrogen, oxygen, water, and carbon dioxide. Such chemical reactions depend on gas diffusion through a material and are either to supply a reactant or to remove products. It can be divided into two categories: permeation-controlled diffusion and reaction-controlled diffusion. For the permeation-controlled reaction, the surface concentration is determined by the solubility of the molecules in the material and the pressure of the applied gas,

$$C_s = S\,p^{\,n} \tag{2.3}$$

where n = 1/2 for dissolution of diatomic gases into metals (Sievert's Law), where dissociation of the molecule occur; or n = 1 for dissolution of atoms or molecules into most dielectrics (Henry's law), where no dissociation take places.

2.1.2 Transport of gases in inorganic glasses

Silicon dioxide (silica) is one of the most commonly encountered substances in both daily life and in electronics manufacturing [6, 7]. From a technological point of view, silica is one of the most useful large-gap materials. Silica plays a crucial role in silicon-based electronic devices, as well as in the glass and ceramic industry. From a geological point of view, silica is one of the main constituents of the earth's crust and mantle, and the investigation of the properties and applications of silica is of fundamental interest.

Vitreous silica is the glass consisting of almost pure SiO_2, which is a key material for fiber optics communication technology and science. The common definition of glasses compared with crystalline materials is regarding their order. The chemical bonding in crystalline silica shows the ordered regularity of a lattice, whereas vitreous silica has more the appearance of a random network, as shown in Fig. 2.2.

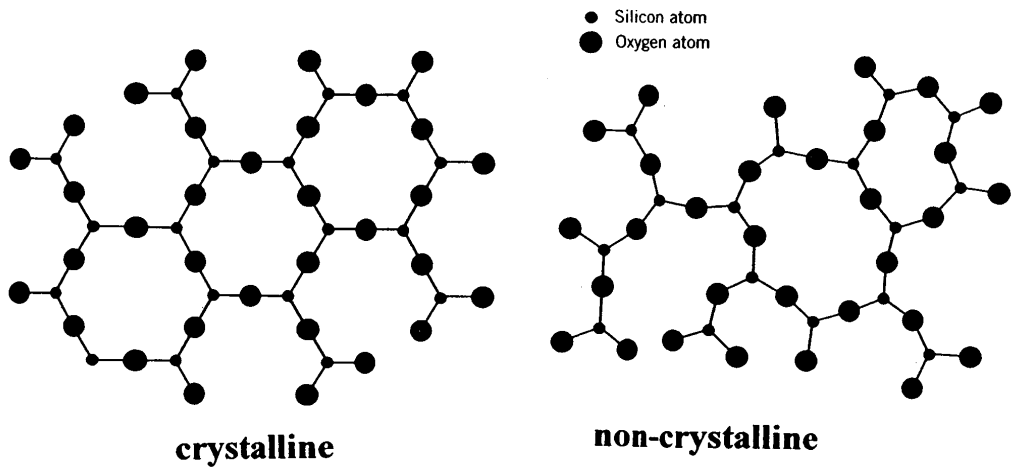

Fig. 2.2 Structure comparison between crystalline and non-crystalline of silica.

Diffusion of gases in glass can be treated as a "random walk" of atoms or molecules through the interstices of the network. The permeation and diffusion of gases in glasses can occur either with or without reaction between the diffusing species and the amorphous network. Diffusion of inert gases occurs without any chemical interaction with the glass. Diffusion of hydrogen, nitrogen, oxygen, or water may or may not involve chemical reactions, depending on the temperature of the materials and the composition of materials. For example, hydrogen diffuses in vitreous silica as molecules at room temperature. At high temperatures or in the glasses containing defects, significant chemical reaction can take place.

Diffusion of gases in glass is influenced by several experimental variables such as temperature, pressure, stress, and volume relation. Studies of the effect of temperature on the diffusivity of helium in vitreous silica demonstrate a traditional Arrhenius expression [3, 8],

$$D = D_0 \, exp\left(\frac{-\Delta H}{RT}\right) \tag{2.4}$$

where D_0 is a constant, ΔH is the enthalpy of activation, R is the gas constant, and T is the temperature.

The diffusivity of monatomic gases should be independent of the partial pressure of those gases in the atmosphere surrounding the specimen under ideal conditions. The flux of a monatomic gas through a specimen should vary linearly proportional to the partial pressure of the gas. It was found that the diffusivity of helium and neon are constant for pressure less than 1 atm within common accuracy [9]. It is not the case at higher pressure because the solubility exhibits saturation behavior.

The diffusion and solubility of gas are dependent on the free volume of the structure, the thermal history of the specimen, and volume relaxation of glasses, especially in case of the measurement at high temperatures.

2.1.3 Transport of gases in ceramics

Gas diffusion in crystalline ceramics with a minimum of a vitreous phase can by either diffusion through an amorphous boundary phase or diffusion through the crystalline lattice itself, and former is considerably faster than that the latter [10, 11]. Gas diffusion varies dramatically with microstructure of sintered materials, such as amount of amorphous phase, size of grain and grain boundary, porosity, and impurity concentration. Lattice diffusion mainly takes place through the movement of point defects. The presence of different types of defects gives rise to different mechanisms of diffusion.

- Vacancy mechanism

The diffusion takes place by the vacancy mechanism if an atom on a normal site jumps into an adjacent vacancy, as schematically illustrated in Fig. 2.3. It should be noted that the atoms move in the direction opposite the vacancies.

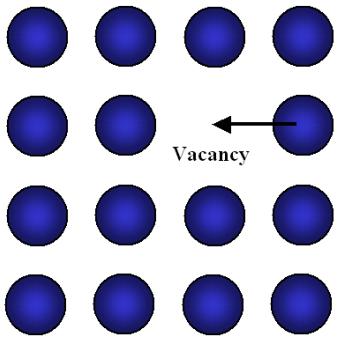

Fig. 2.3 Schematic illustration of vacancy diffusion in lattice.

- Interstitial mechanism

If an atom on an interstitial site moves to one of the neighboring interstitial sites, the diffusion occurs by an interstitial mechanism, as schematically shown in Fig. 2.4. Such a movement or jump of the interstitial atom involves a considerable distortion of the lattice, and this mechanism is probable when the interstitial atom is smaller than the atoms on the normal lattice positions.

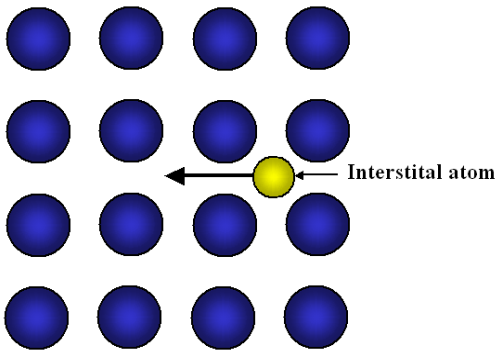

Fig. 2.4 Schematic illustration of interstitial diffusion in lattice.

- Interstitialcy mechanism

In the interstitialcy mechanism an interstitial atom pushes one of its nearest neighbors on a normal lattice site into another interstitial position and itself occupies the lattice site of the displaced atom. This mechanism takes place if the distortion becomes too large to make the interstitial mechanism probable, as schematically illustrated in Fig. 2.5.

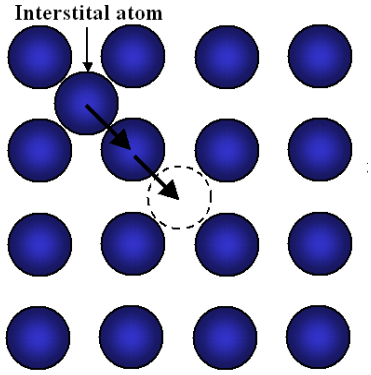

Fig. 2.5 Schematic illustration of interstitialcy diffusion in lattice.

2.2 High temperature oxidation of metals

2.2.1 Mechanisms of oxidation kinetics

Knowledge of reaction rates and kinetics for a metal is important for elucidation of oxidation mechanisms. Rate equations are commonly classified as linear, parabolic and logarithmic [12-14], as schematically shown in Fig. 2.6 and Fig. 2.7, respectively.

- Linear rate equation

Linear oxidation is described by

$$x = k_l t \tag{2.5}$$

where x is oxidation growth and may alternatively represent the thickness of the oxide film, the amount of oxygen or metal consumed in the oxidation, etc., t is the time, and k_l is the linear rate constant. If the rate is linear, surface or phase boundary process or reaction may be rate determining. This may involve a steady state reaction limited by the supply at the surface, a reaction governed by a steady state formation of oxide at the metal-oxide interface, or diffusion through a protective layer with constant thickness.

The linear oxide growth may arise in another way. If the oxide film is formed in a strained condition, it may, at high temperature, keep breaking down or flaking off as quickly as it is formed.

Example of this phenomenon is that chromium which shows a sudden speeding up of the oxidation rate at a certain thickness. On chromium, in the range of 950-1050°C, the increase in oxidation often occurs when the thickness reaches 480 nm; above 1050°C, a second increase occurs about 420 nm [15]. On nickel, the films often crack away from the metal at 1000°C [16].

- Parabolic rate equation

Parabolic oxidation is described by

$$x^2 = k_p t \tag{2.6}$$

where k_p is the parabolic rate constant. It indicates a thermal diffusion process, which include a uniform diffusion of one or two reactants through a growing scale, or a uniform diffusion of gaseous reactant into the metal.

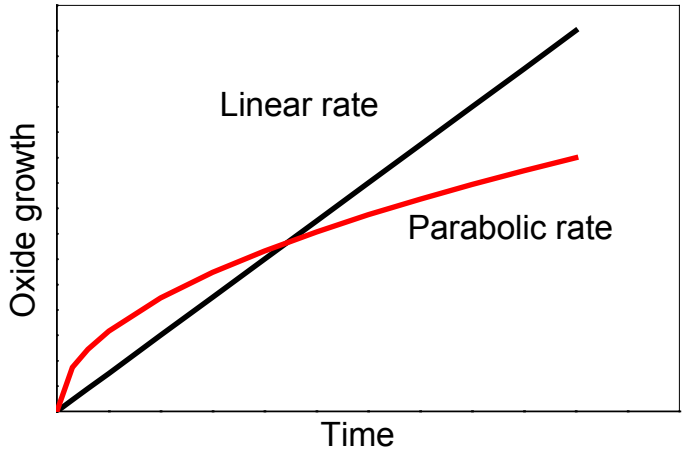

Fig. 2.6 Schematic illustration of oxide growth versus time for linear and parabolic oxidation.

- Logarithmic rate equation

It is characteristic of the oxidation of many metals at low temperatures (general below 300 - 400°C) where the reaction is initially quite rapid and then drops off to low or negligible rates. The behavior is often described by a logarithmic rate equation,

$$x = k_{log} \log(t + t_O) + A \quad (2.7)$$

and inverse logarithmic rate equation,

$$1/x = B - k_{ilog} \log(t) \quad (2.8)$$

where k_{log} and k_{ilog} are the rate constants, and A and B are constants.

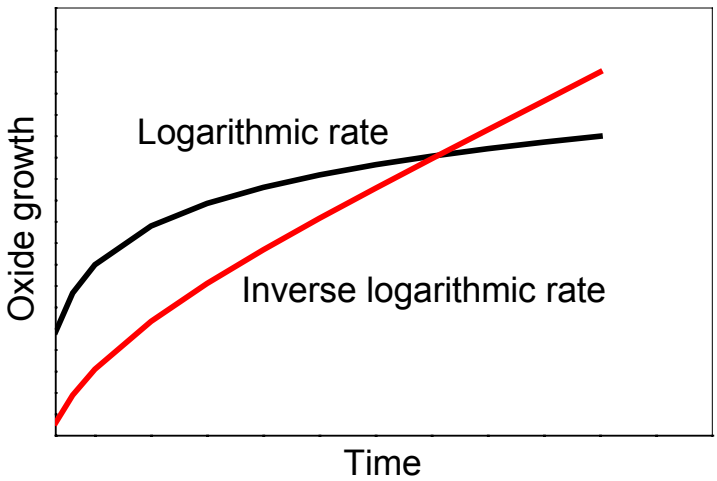

Fig. 2.7 Schematic illustration of oxide growth versus time for logarithmic and inverse logarithmic oxidation.

2.2.2 Classification of metals according to oxidation behavior

The formation of a dense oxide layer on the metal substrate separates the metal and gas phase. If sufficient oxygen is available at the oxide surface, the oxidation rate at high temperature will be limited by solid-state diffusion of the reactants or electrons through the oxide layer. The oxidation rate decreases with time as the oxides layer grows in thickness due to the increasing length of diffusion paths.

The solid-state diffusion of the reactants takes place by various mechanisms: diffusion via the lattice and along grain boundaries and other easy diffusion paths such as pores and cavities. Wagner oxidation theory uses an ideal model that the oxide scale is dense and continuous and adheres to the metal [17-19]. This theory assumes that the lattice diffusion of reacting atoms or ions or the transport of electrons through the dense oxide layer is rate determing in the overall oxidation reaction. Lattice diffusion can take place because of the presence of the point defects, and the migrating species may alternatively be considered to constitute lattice and electronic defects, e.g. vacancies, interstitial ions and electrons and electron holes, which have been mentioned mostly in Section 2.1.3. The overall driving force of the reaction is the free energy change associated with the formation of oxides from the metal and the oxygen. For such a reaction mechanism, the oxidation rate is parabolic with time, as mentioned in Section 2.2.1.

It has been found that the diffusion along grain boundaries and dislocations are much faster than that in the bulk [20]. For a non-gas tight oxide layer, molecular oxygen diffuses through pores and cavities, which are studied in attached papers. In practice, due to the complexity of cooperation of several mechanisms, these cannot be integrated exactly, and only approximations for the oxide growth rate as a function of time can be obtained. This makes the experimental verification of theory based only on the measurements of the oxidation kinetics difficult. However, the use of tracer atoms (both metal and oxygen) provides valuable information on the transport mechanism (e.g. migrating species) in the oxidation process, and can be a useful tool for the experimental test of theory. The tracing of oxygen species is usually performed by oxidation first in $^{16,16}O_2$ and then $^{18,18}O_2$ enriched gas. Oxidation mechanisms can be investigated by a subsequent SIMS depth profiling of the oxide. There are three possible growth modes of oxide formed on the substrate of metals.

- Oxide film formed by outward movement of metal ions

In this case, the growth of oxide films occurs by outward movement of metal ions and takes up the positions between oxygen on the external face to form fresh layer of oxides, as shown in Fig. 2.8(a). There is no risk for the development of any large compressive strain in the film, since the metal ions on arrival are free to take up positions of minimal

energy. At the same time, the movement of metal ions from the metal substrate into the film leaves vacancies at the interface and this may coalesce to form cavities. Examples are the oxidation of iron, zinc, and nickel.

- Metals forming oxide films by inward movement of oxygen ions

It is shown in Fig. 2.8(b). If an oxide film is formed on a metal by oxygen moving inwards, it is likely that the oxide will be in a state of strain due to a volume-relation of oxide and metal. The film will have stress-distribution tending to make it curl up when it is loosened from metallic basis. Examples are the oxidation of titanium, and zirconium.

- Simultaneous movement in both directions

It is shown in Fig. 2.8(c). It has been shown that movement of anions inwards tends to mostly produce compressive stress, while movement of cations outwards tends to produce cavities. However, in many cases where either stress or cavities may reasonably be expected, they do not appear; instead there is a plastic yield of the film. One possibility is that this result may be connected with movements in both directions. If cations move in sufficiently to avoid the development of stress and anions move in sufficiently to avoid the development of cavities, a highly resistant film should develop, which was suggested by U. R. Evans in 1963 [21]. Then the interesting question is how to realize the simultaneous movement in both directions.

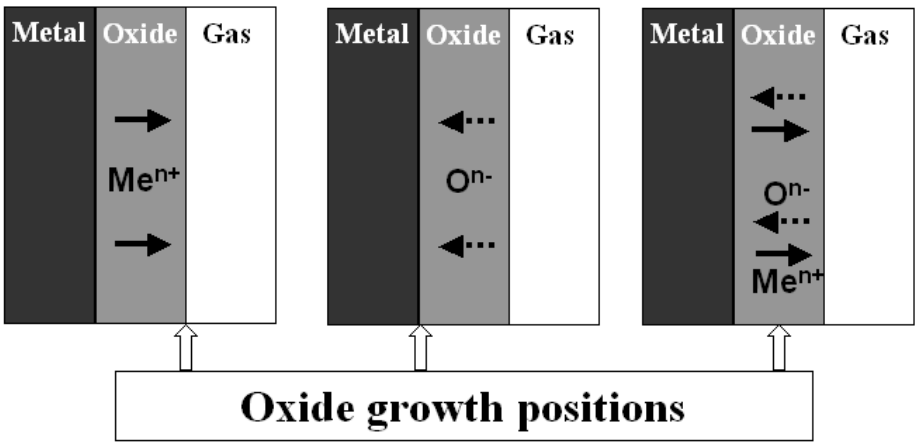

(a) (b) (c)

Fig. 2.8 The mechanisms of oxide growth on metal subtracts.

It has been found by the work performed at our division that the mechanisms of oxide growth can be manipulated by changing the hydrogen content in materials and by applying the oxygen dissociating elements (ODEs) including Pt, yttria and ceria. The hydrogen in metals and oxides influences the transport of metal cations in oxides formed

on the metallic substrates [22-26]. Applying a small amount of ODEs to the surface or in the materials can enhance the transport of dissociated oxygen in oxides [25, 27-29], which I have looked in details in this thesis.

Due to the identification of "tools" for influencing metal-ion transport by controlling hydrogen in gas and substrate and for influencing oxygen-ion transport by using ODE, the old suggestion could be tested and the concept of self-repairing metal-oxides was introduced [30]. An illustration of how hydrogen and oxygen dissociating elements influence the growth of oxides is shown in Fig. 2.9. Here the hydrogen and ODE can be used to obtain a beneficial balance between metal ions and oxygen ions. A balanced transport facilitates an oxide growth at both the substrate-oxide interface with improved scale adherence, and at oxide-gas interfaces with reduced risk for crack formation. Furthermore, the situation of a balanced metal ion and oxygen ion transport is a prerequisite for oxide growth within the metal-oxide itself. If this oxide growth takes place in pores and other imperfections we have a situation/position of a self-repairing metal-oxide.

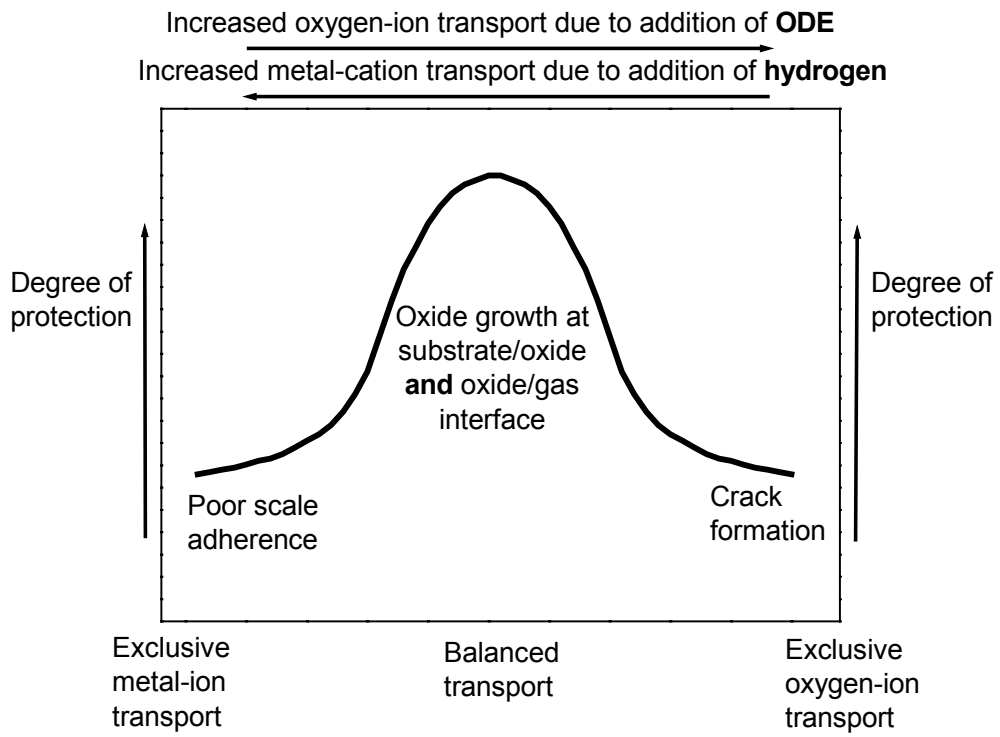

Fig. 2.9 Change of oxide growth position(s) and corresponding degree of metal protection due to ODE and hydrogen addition. The additions are indicated by arrow at the top of the diagram. Exclusive metal-cation transport leads to oxide growth at oxide-gas interface and exclusive oxygen-anion transport leads to oxide growth at substrate-oxide interface [30].

References

1. J. E. Shelby, Molecular Solubility and Diffusion. Ch. 1. Treatise on Materials Science and Technology. Vol 17: Glass II. Ed. By M. Tomozawa and R. H. Doremus, Academic Press. New York, 1979
2. J. Crank, The Mathematics of Diffusion, 2nd edition, Clarendon Press, Oxford, 1975
3. D. E. Swets, R. W. Lee, and R. C. Frank, J. Chem. Phys., 34 (1961), 17
4. R. S. Wortman and J. f. Shackelford, J. Non-Cryst. Solids, 125 (1990), 280
5. J. E. Shelby, J. Appl. Phys., 47 (1976), 135
6. R. Bruckner, J. Non-Crystal. Solids, 5 (1970), 123
7. R. Bruckner, J. Non-Crystal. Solids, 5 (1970), 177
8. J. E. Shelby, J. Am. Ceram. Soc., 54 (1971), 125
9. J. E. Shelby and S. C. Keeton, J. Am. Ceramic. Soc., 57 (1972), 45
10. J. E. Shelby, J. Non-Cryst. Solids, 43 (1981), 255
11. J. E. Shelby and M. C. Nichols, J. Am. Ceram. Soc., 66 (1983), 200
12. U. R. Evans, The Corrosion and Oxidation of Metals, Edward Arnold, London, 1960
13. P. Kofstad, High-Temperature Oxidation of Metals, Wiley, New York, 1966.
14. O. Kubaschewski, and B. E. Hopkins, Oxidation of Metals and Alloys, Butterworths, London, 1962.
15. U. R. Evans, The Corrosion and Oxidation of Metals: Scientific Principles and Practical Application. Edward Arnold LTD, London, 1960
16. E. A. Gulbransen and K. F. Andrew, J. Electrochem. Soc., 104 (1957), 334
17. C. Wagner, Atom Movements, American Society Metal, pp.153, Cleveland, OH, 1951
18. C. Wagner, Prog. Solid. Chem., 10 (1975), 3
19. P. Kofstad, High Temperature Corrosion, pp.162, Elsevier Applied science, London, 1988
20. U. Brossmann, R. Wurschun, U. Södervall, and H. E. Schaefer, J. Appl. Phys., 85 (1999), 7464
21. U. R. Evans, An Introduction to Metallic Corrosion, pp.17, Edward Arnold LTD, London, 1963
22. B. Tveten, G. Hultquist, and T. Norby, Oxid. Met., 51 (1999), 221
23. G. Hultquist, B. Tveten, and E. Hörnlund, Oxid. Met., 54 (2000), 1
24. D. Wallinder, E. Hörnlund, and G. Hultquist, J. Electochem. Soc., 149(2002), B393
25. C. Anghel, G. Hultquist, and M. Limbäck, J. Nuclear. Mater., 340 (2005), 271
26. G. Hultquist, C. Anghel, and P Szakalos, Mater. Sci. Forum, 552-523 (2006), 139
27. G. Hultquist, E. Hörnlund, and Q. Dong, Corros. Sci., 45 (2003), 2697
28. J. Angenete, K. Stiller, and V. Langer, Oxid. Met., 60 (2003), 47
29. G. Hultquist, M. J. Graham, A. T. S. Wee, R. Liu, G. I. Sproule, Q. Dong, and C. Anghel, J. Electrochem. Soc., 153 (2006), G182
30. G. Hultquist, B. Tveten, E. Hörnlund, M. Limbäck, and R. Haygsrud, Oxid. Met. 56 (2001), 313.

Chapter 3

Experimental

3.1 Summary of experiments

3.1.1 Materials studied

Pt-effects on the oxidation of metals Al, Cr, Ni, Fe, and Zr were performed by using the samples in the absence of Pt, partly coated with porous Pt-films, and coated with porous Pt-films, as schematically shown in Fig. 3.1. Porous Pt-films were coated on the metal substrates by using a Polaron E5400 high-resolution sputter coater with a platinum target. The metals used in this thesis, the sample preparation, and oxidation conditions are given in Table 3.1.

(a) (b) (c)

Fig. 3.1 Metal samples used for oxidation (a) In the absence of Pt; (b) Partly coated with porous Pt-film; (c) Coated with porous Pt-film.

Table 3.1 The metals used in this study, the sample preparation and oxidation conditions.

Sample	Temperature, ^{o}C	Oxidation gas	Pt coating	H content, wt ppm	Paper
Al	600	$^{16,16}O_2 + {}^{18,18}O_2$	Partly	<5	6
Cr	800	$^{16,16}O_2 + {}^{18,18}O_2$	Partly	<5	1
Ni	800	$^{16,16}O_2 + {}^{18,18}O_2$	Partly	5	6
Ni	500	Air	0, 0.8, 2.4, 6.4 μg/cm^2	5	6
Ni	500	Air	0, 8.0, 19.4, 33.6, 50.8, 56.1, 128.5 μg/cm^2	5	6
Ni	500	Air + $^{18,18}O_2$	0, 0.8, 14.2 μg/cm^2	5	6
Zr	400	$^{16,16}O_2 + {}^{18,18}O_2$	Partly	<5	6

Oxides studied are those formed on Fe- and Zircaloy-2-substrates, vitreous silica, and yttria stabilized zirconia (YSZ), as listed in Table 3.2.

Table 3.2 Characterization of the oxides used in this study.

Sample	Shape	Experiment	Paper
Oxide on Fe	Plate	Uptake/release	4
Oxide on Zircaloy-2	Plate	Uptake/release	4
Vitreous silica	Tube	Permeation, Uptake/release	2, 3
Yttria-stabilized zirconia	Tube	Permeation, Uptake/release	7, 8

3.1.2 Gases used

The gases used in the transport study of gases in oxides together with the experiment conditions are summarized in Table 3.3.

Table 3.3 Experimental conditions of gas transport in oxides

Gas	T, ^{o}C	P_{tot}, mbar	Material	Experiment	Paper
H_2	550	70-1200	Vitreous silica	Permeation	2
N_2 with 60 % ^{15}N	900	225	Vitreous silica	Permeation	3
N_2 with 50 % ^{15}N	25, 200, 550, 900	400	Vitreous silica	Uptake/release	3
$1/4O_2+1/4N_2$ $+1/4Ar+1/4He$	25 (uptake) 25- 900 (release)	1000	YSZ	Uptake/release	7
O_2 with 93% ^{18}O	600, 700, 800, 900	20	YSZ	Uptake/release	7, 8
N_2 with 60 % ^{15}N	950	110	YSZ	Permeation	7
H_2 with 47% ^{2}H	25	640	YSZ	Permeation	7
$1/4O_2+1/4N_2$ $+1/4Ar+1/4He$	400, 600, 800, 900, 950, 980	1000	YSZ	Permeation	7
Air	200, 400, 600, 800, 900, 950	480	YSZ	Permeation	7

3.2 Gas Phase Analysis (GPA)

Fig. 3.2 shows schematically the equipment used to study transport in oxides. It consists of three main parts: an enclosed reaction chamber of approximately 70 cm^3, a mass spectrometer (MS) placed in an ultra high vacuum (UHV) chamber with an ion pump and a gas handling system containing a rough pump. These three parts are joined with

stainless steel couplings. A tube furnace that can be moved back and forth on a rail and it provides temperatures in the range of 25-1200°C.

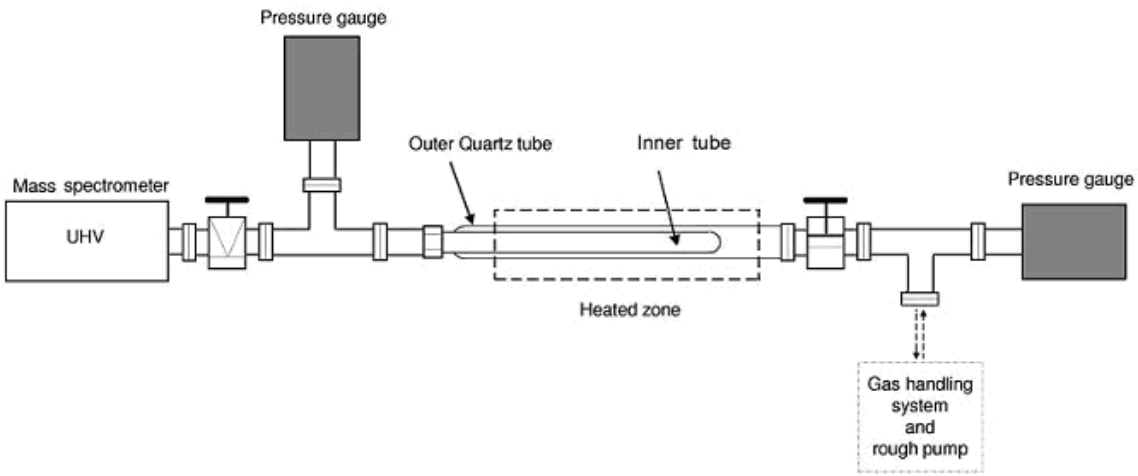

Fig. 3.2 Gas Phase Analysis experimental setup.

The GAP technique offers a versatile tool for studying many different processes. Reactions taking place on a sample are studied by analyzing the gas in the closed reaction chamber. The equipment is basically used in two modes:
The first mode is used to monitor the release of gaseous components from samples. Gases released from a sample are analyzed by the MS and evacuated by the ion pump. By calibration of MS signal and the ion pump speed [1], the gaseous components released from a sample can be measured. A typical example of measurement in this mode is outgassing from different materials.
In the second mode, the reaction chamber is filled with gas from the gas handling system and the leak valve connected to the MS is either closed or slightly opened to probe the gas composition. The probing enables measurements of isotopic exchange due to different reactions. The consumption of gas due to probing is generally negligible in comparison with the gas consumption due to reaction with the sample. Typical measurements in this mode are oxide formation, hydrogen uptake and calculation of dissociation rates.

In attached papers, GPA is used for the following measurements and experiments.

3.2.1 Two-stage oxidation

Two-stage oxidation is performed by two consecutive exposures of the sample and the oxygen isotope is changed. For example oxidation in $^{16,16}O_2$ followed by oxidation in $^{18,18}O_2$, as illustrated in Fig. 3.3. By SIMS analysis of the oxide formed in the two-stage oxidation, information about oxide growth processes is obtained. If the oxide grows exclusively by metal transport, the isotope used in the second stage of oxidation appears at

the oxide-gas interface. If the oxide grows exclusively by oxygen transport and exchange with oxygen is negligible, then the isotope used in the second stage of the oxidation is found at the oxide-metal interface. By using a mixture of $^{16,16}O_2$ and $^{18,18}O_2$ in the second stage, information about molecular dissociation rates and isotopic exchange rates with the oxide may be retrieved.

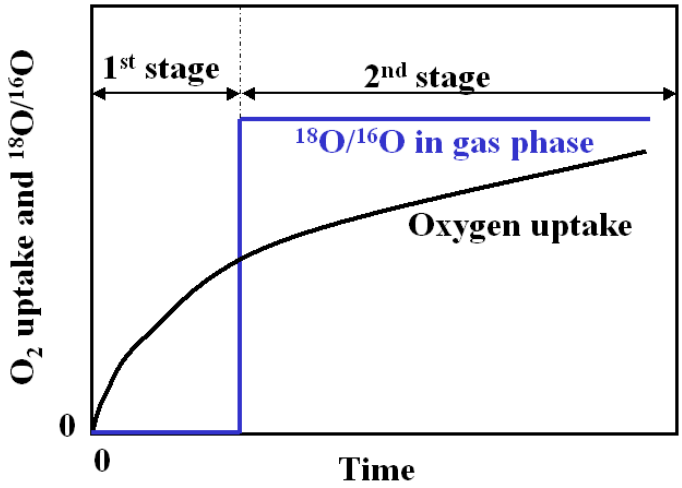

Fig. 3.3 Schematics of two-stage oxidation of metals.

3.2.2 Permeation measurement

Permeation measurement is performed by using a membrane, as illustrated in Fig. 3.4. The experimental procedure for flux measurement is as follows: the membrane is held at a certain temperature sufficiently long to provide a constant low background of gas. At zero time, a known pressure of gas is introduced into the outer volume. The flux of gas through the membrane is continuously monitored by the mass spectrometer. Steady-state flux of gas is judged when virtually no further increase of signal in the mass spectrometer can be seen.

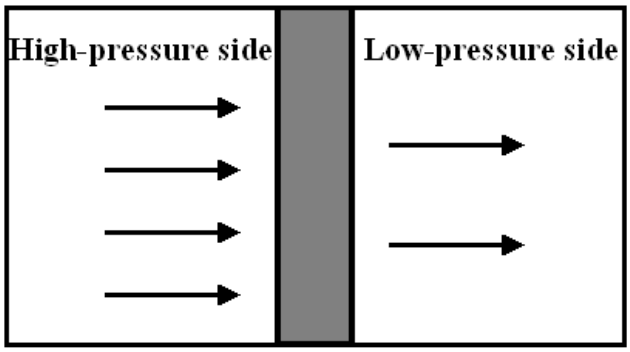

Fig. 3.4 Schematics of permeation measurement.

3.2.3 Uptake/release measurement

Uptake/release measurement is performed by exposure a sample to a known gas in a closed volume following by outgassing the material, as illustrated in Fig.3.5. The outgassing of gas from the sample is carried out in the following way. After steady state has been established, the influx gas is evacuated by the rough pump, and the specimen is heated by the furnace rapidly. The aim of this procedure is that the concentration profile in the material created at steady state diffusion remains when the outgassing starts. A decay curve was obtained for the release of gas into the mass spectrometer system. The concentration of gas can be obtained by integrating the flux during the decay process over time to yield the total amount of gas released from the sample.

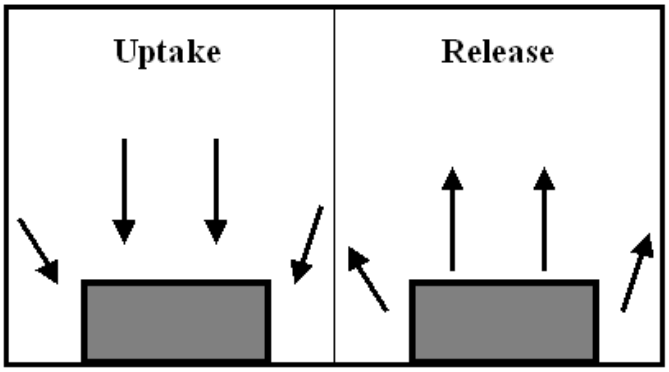

Fig. 3.5 Schematics of uptake/release measurement.

3.3 Secondary Ion Mass Spectrometry (SIMS)

SIMS is a mass- and isotope-sensitive spectroscopic method. The surface of a sample is placed in UHV and sputtered with an ion beam [2]. Fragments in the form of both negative and positive secondary ions and neutral species are knocked off from the sample surface. As the name of the method indicates, the secondary ions are analyzed. The detection limit of SIMS is often in the ppm range.

SIMS is widely used for analysis of trace elements in solid materials, especially semiconductors and thin films. The SIMS primary ion beam can be focused to less than 1μm in diameter. Controlling the location where the primary ion bean strikes the sample surface permits microanalysis; the measurement of the lateral distribution of elements on a microscopic scale can be done. Continuous analysis with a MS while sputtering produced information as a function of depth, called a depth profile. When the sputter rate is extremely slow, the analysis can be performed while consuming less than a tenth of an atomic monolayer. This slow sputtering mode is called static SIMS to separate it from dynamic SIMS used for depth profiles. In the work presented in this thesis, only dynamic SIMS has been used. The SIMS technique is very useful to analyze samples exposed to

rare isotopes. The growth mode of an oxide (metal or oxygen transport) can be determined by a two-stage oxidation followed by a depth profile in SIMS.

The main advantages of SIMS are the possibility to detect hydrogen, different isotopes, and the low detection limit (in the ppm range). The main drawback is the difficulty to quantify SIMS data, due to the complexity of the ionization process.
In the present studies, the samples were often coated with gold in vacuum before they were introduced into the SIMS apparatus, to avoid difficulties with charging of the sample.

3.4 X-ray Photoelectron Spectroscopy (XPS)

X-ray photoelectron spectroscopy is one of the most widely used methods for surface analysis and the main reason is that the interpretation is well established [3-4]. The measured parameter is the kinetic energy of electrons ejected from the atoms upon X-ray radiation.

$$E_{kin} = h\nu - E_b - \Phi \qquad (3.1)$$

Where E_{kin} is the kinetic energy of the electrons, $h\nu$ is the energy of the X-ray radiation, E_b is the binding energy of the electrons to the atoms, and Φ is the work function of the spectrometer. Different elements have different binding energies, therefore, element identification (both concentration of elements and their chemical states) is possibly analyzed by XPS.
One advantage with XPS compared to SIMS is that the composition of the surface can be determined. The disadvantage is that hydrogen is not directly detectable. Hydrogen bonded to other species gives a chemical shift in theses species, but the interpretation of this shift is not straightforward.
The intensity of the signal from an oxide layer depends on mean free path of detected electrons and the thickness of oxide. The probing depth is 1-3 nm for studied oxides.

3.5 Scanning Electron Microscopy (SEM)

In scanning electron microscopy an electron beam is scanned over an area of the sample surface, and electros emitted from the surface are collected and amplified to form a video signal. FEG-SEM analysis was performed with a Leo 1530 Field Emission Scanning Electron Microscope equipped with a GEMINI field emission column.

References

1. T. Åkermark, G. Hultquist, and Q. Lu, J. Mater. Eng. Perf., 5 (1996), 516
2. J. C. Vickermann, A. Brown, and N. M. Reed, Secondary Ion Mass Spectrometry, Craendon Press-oxford, 1989
3. J. F. Moulder, W. F. Stickler, P. E. Sobol, and K. D. Bomben, Handbook of X-ray Photoelectron Spectroscopy. J. Chastain (Ed.) Perkin-Elmer Corporation, Minnesota, 1992
4. D. Briggs and M. P. Seah, Practical Surface Analysis, (Sec. Ed.) volume 1, Auger and X-ray Photoelectron Spectroscopy, John Wiley &Sons, Chichester, 1994

Chapter 4

Summary of appended papers

The main results from papers 1- 8 are briefly described and discussed topic by topic.

4.1 A gas phase analysis technique applied to in-situ study of gas-solid interactions (Paper 5)

This paper is a comprehensive introduction of Gas Phase Analysis, which is a straightforward and reliable technique and based on mass spectrometry and labeled gases. The technique has been used to study in-situ gas-solid interactions. This technique can be used at temperatures from room temperature to 1200°C and at pressures up to about 1 atm.

The following principles of measurements on chemical reactions (oxidation, hydration) between solids and gas mixtures by use of gas phase analysis are described: the oxidation mechanisms with use of oxygen isotopes, effects of hydrogen on the corrosion mechanisms of metallic materials, the dissociation of gases molecules on solid surfaces, and isotopic exchange between the molecules from the gas phase and the atoms in the lattice.

Outgassing of solid materials that is to quantify the amount of gas release after exposure of samples to studied gases, and permeation of gases through membranes are summarized and the experimental arrangements are explained in details in this paper. Examples are selected for each type of measurement: oxidation of Fe in oxygen at 900°C and oxidation of Zircaloy-2 in oxygen at 400-500°C, outgassing of air equilibrated Zr-based oxide scales at 80°C and oxygen permeation through an YSZ membrane at 400-980°C. Oxygen dissociation rates on solid surfaces are measured by use of this technique in 20 mbar oxygen at temperatures 200-900°C and summarized in Fig. 4.1. It indicates that at lower temperatures, the difference among the oxygen dissociation rates on these materials is considerable. Oxide formed on Ru is the best catalyst for oxygen dissociation, and quartz shows the low oxygen dissociation efficiency, which makes it to be ideal as a reaction chamber material.

By combining GPA with another isotopic sensitive technique such as SIMS, the measured changes in composition of gas phase can be retrieved by analyzing the reaction products. Aspects related to sample preparation that includes surface preparation, surface coating, and hydrogen or deuterium charging of samples, isotopic gas mixture selection, data

acquisition, calibration of mass spectrometer, and interpretations of the experimental data are also addressed in this paper.

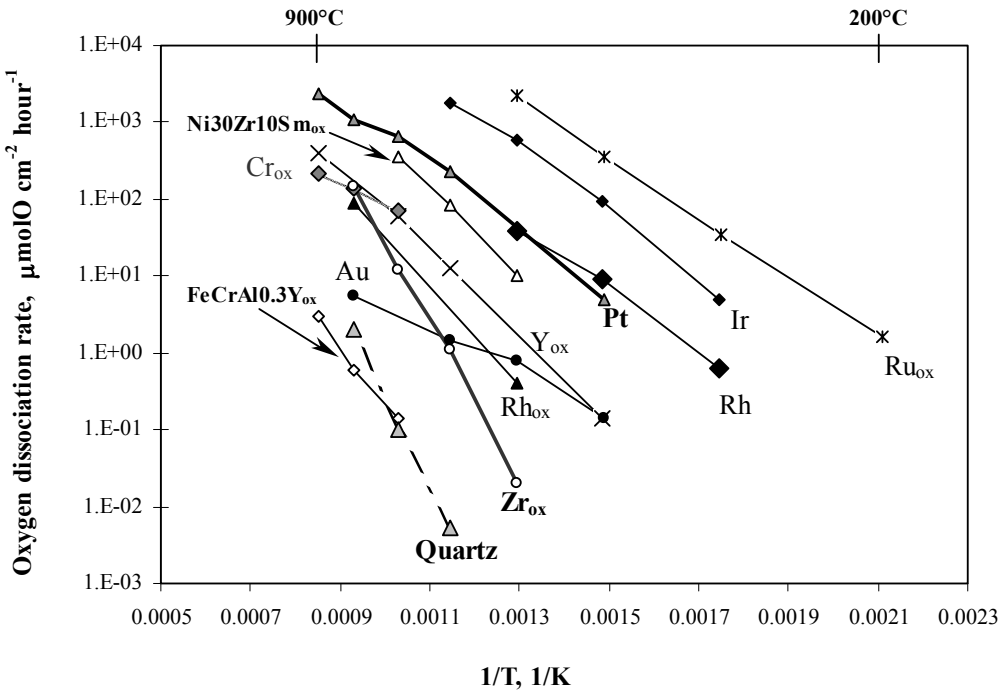

Fig. 4.1 oxygen dissociation rate on various materials in 20 mbar O_2 versus 1/T.

4.2 An experimental method to identify different species of gases and their contribution to the overall transport of gases in oxides (Papers 3 and 8)

Transport of gases in oxides may take place in molecular, atomic, and ionic form. Exposure of oxides to isotopic labeled gas and measurements of the change of abundance of isotopes among molecules in gas phase is a possible way to identify the diffusing molecules, atoms, ions and to evaluate their contribution to the overall oxygen transport in oxides.

Two types of experiments, permeation and uptake/release, may be performed. Taking the study of oxygen transport in oxide by uptake/release measurement as example, an exclusive molecular oxygen transport, exclusive atomic oxygen transport and exclusive ionic oxygen transport in an oxide at the beginning of exposure and after outgassing are illustrated in Fig. 4.2. In this figure the oxide containing $^{16}O^{2-}$ and vacancies exposed to oxygen isotopes with 50% $^{16,16}O_2$ and 50% $^{18,18}O_2$ at zero time in Fig. 4.2(a). It is assumed the composition change of gas during exposure is negligible. In case of exclusive molecular transport, the composition of released oxygen is the same as that in the

exposure because no dissociation and also no exchange have taken place, as illustrated in Fig. 4.2 (b). In case of exclusive atomic transport, oxygen molecules dissociate and associate on the surface of the oxide resulting in a statistically equilibrated oxygen composition in the released gas, and the abundance of ^{18}O (as well as ^{16}O) in gas phase is constant, as illustrated in Fig. 4.2(c). In case of exclusive ionic transport, all oxygen from gas phase exchanges with $^{16}O^{2-}$ in the oxide lattice, which leads to a gas release of $^{16,16}O_2$, as illustrated in Fig. 4.2(d).

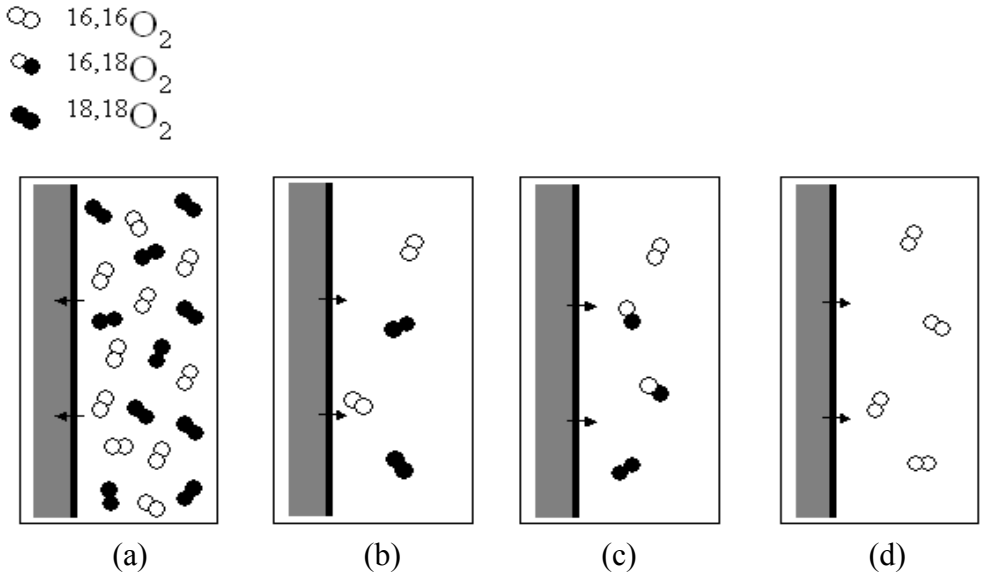

Fig. 4.2 Schematics of exclusive molecular transport (O_2), exclusive atomic transport (O), and exclusive ionic transport (O^{2-}) in oxide containing $^{16}O^{2-}$ and oxygen vacancies with exposure to oxygen isotopes (50% $^{16,16}O_2$ + 50% $^{18,18}O_2$). (a) Exposure at zero time, (b) Exclusive molecular transport, (c) Exclusive atomic transport, (d) Exclusive ionic transport (Paper 8).

The procedure to calculate the contributions of ionic, molecular, and atomic oxygen transport to the total oxygen transport is calculated by using the abundance of ^{16}O and ^{18}O by the following ways:

$$\% \text{ ionic transport } (O^{2-}) = \frac{f16_{release} - f16_{exposure}}{f18_{exposure}} \cdot 100 , \qquad (4.1)$$

where $f16_{exposure}$ and $f16_{release}$ are the fraction of ^{16}O in exposure and at release, respectively, where $f16 = \frac{[^{16}O]}{[^{16}O]+[^{18}O]}$; $f18_{exposure}$ is the fraction of ^{18}O in exposure, where $f18 = \frac{[^{18}O]}{[^{16}O]+[^{18}O]}$.

The decrease in abundance of $^{18,18}O_2$ and the increase in abundance of $^{16,16}O_2$ or $^{16,18}O_2$ in the gas phase are due to non-molecular (atomic and ionic) transport. The percentage of

molecular oxygen transport is calculated by using the abundance of $^{18,18}O_2$ in exposure gas, released gas and gas at statistical equilibrium,

$$\% \text{ molecular transport } (O_2) = \frac{f36_{release} - f36_{equilibrium}}{f36_{exposure} - f36_{equilibrium}} \cdot 100, \qquad (4.2)$$

where $f36_{exposure}$, $f36_{release}$, and $f36_{equilibrium}$ are the fraction of $^{18,18}O_2$ in exposure, release, and at statistical equilibrium, respectively, where $f36 = \frac{\left[{}^{18,18}O_2\right]}{\left[{}^{16,16}O_2\right] + \left[{}^{16,18}O_2\right] + \left[{}^{18,18}O_2\right]}$. $f36_{equilibrium}$ is calculated based on the abundance of ^{16}O and ^{18}O isotopes at release.

$$\% \text{ atomic transport } (O) = 100\% - \% \text{ ionic transport } (O^{2-}) - \% \text{ molecular transport } (O_2), \qquad (4.3)$$

In the general case, exposure to non-equilibrated O_2 containing 60-70 % ^{18}O is optimal to obtain the highest accuracy in the measurement. The method is exemplified by identifying molecular, atomic, and ionic oxygen transport in a commercial yttria stabilized zirconia sample in the temperature range of 600-900°C in Paper 8. It is found that there is approximately 35% molecular, 19% atomic transport, and 46% ionic oxygen transport in YSZ at 600°C. The fraction of ionic oxygen transport increases with increasing temperature, and that of non-ionic oxygen transport decreases with increasing temperature, as seen in Fig. 4.3.

Study of nitrogen transport in vitreous silica by permeation measurements is another example given in Paper 3 that the method applied. It is concluded that nitrogen diffuses both in molecular and atomic form in vitreous silica with approximately 85% molecular and 15% atomic nitrogen transport at 900°C.

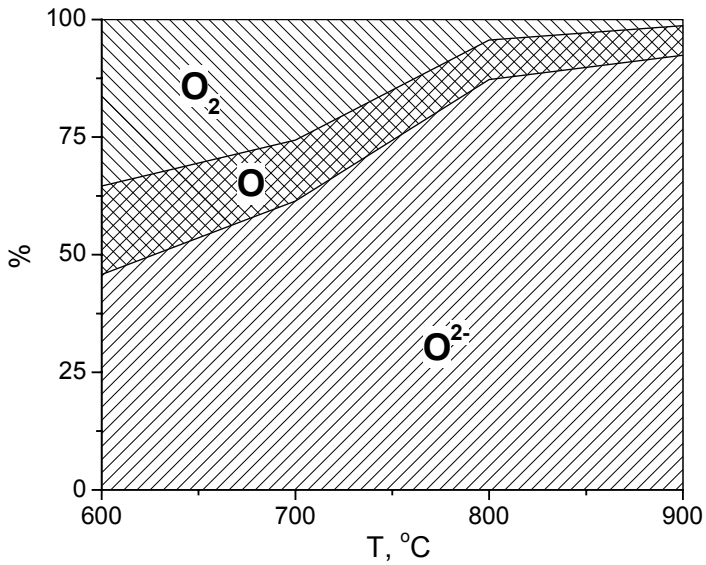

Fig. 4.3 Contributions of molecular (O_2), atomic (O) and ionic (O^{2-}) transport to the overall oxygen transport in the YSZ tube versus temperature (Paper 8).

4.3 A method for evaluation of diffusion parameters of gases in porous oxides (Paper 4)

A novel and relatively straightforward method to quantify diffusion and the amount of gas present in oxide scale on samples equilibrated in controlled atmosphere is presented in Paper 4. A mathematical model for calculation of diffusivity and gas content is given for plate geometry.

The flux from a single surface of the plate is expressed by the formula,

$$F = \frac{2DC_1}{L}\sum_{n=1}^{\infty} exp\left[-(2n-1)^2\pi^2\frac{Dt}{4L^2}\right] \tag{4.4}$$

where F is the flux, D is the diffusivity, C_1 is the concentration, t is the time, L is the thickness of plate.

The magnitude of the terms of the series decreases with n, and in a long time experiment only the first term is significant. This means that in an ${}^{e}\log F$ versus t diagram the flux approaches an asymptote in the form of a straight line of slope when t gets long. A first measurement value of the outgassing experiment is the absolute value of the asymptotic slope of Eq. (4.5),

$$m_1 = \frac{\pi^2 D}{4L^2} \tag{4.5}$$

When the asymptote is drawn backward in time as a straight line, it intersects the diagram axis $t = 0$ at the value ${}^{e}log[2DC_1/L]$. Calculating the exponential of the value on intersection, one gets a second measurement value,

$$m_2 = \frac{2DC_1}{L} \tag{4.6}$$

For a given size L, C_1 and D are determined by the values m_1 and m_2. The third measurement value is the total amount of outgassed substance obtained from flux integration,

$$m_3 = LC_1 \tag{4.7}$$

For completeness, measurement values are given for two-sides release from a plate on the assumption of a uniform concentration C_1. On doubling the flux expressed by Eq. (4.4) one obtains for gas release,

$$m_1 = \frac{\pi^2 D}{l^2} \tag{4.8}$$

$$m_2 = \frac{8DC_1}{l} \tag{4.9}$$

Using the above-described method, the diffusion parameters of He at 80°C in a vitreous silica plate of thickness l = 0.1 cm after equilibration in an exposure to 250 mbar He was investigated. The flux is depicted in the Fig. 4.3. The horizontal axis is time t, and the

vertical axis is flux F expressed in powers of ten corresponding to the proper logarithmic scale ${}^{e}\log F$. The parameters m_1 and m_2 are obtained from Fig. 4.4. He diffusivity is thereby calculated using Eqs. (4.8) and (4.9) and the results are presented in Table 4.1. Fig. 4.5 is obtained by integrating the flux data from Fig. 4.4 over time. The concentration of He in the material is calculated by Eqs. (4.7) and (4.9) and the result is also presented in Table 4.1.

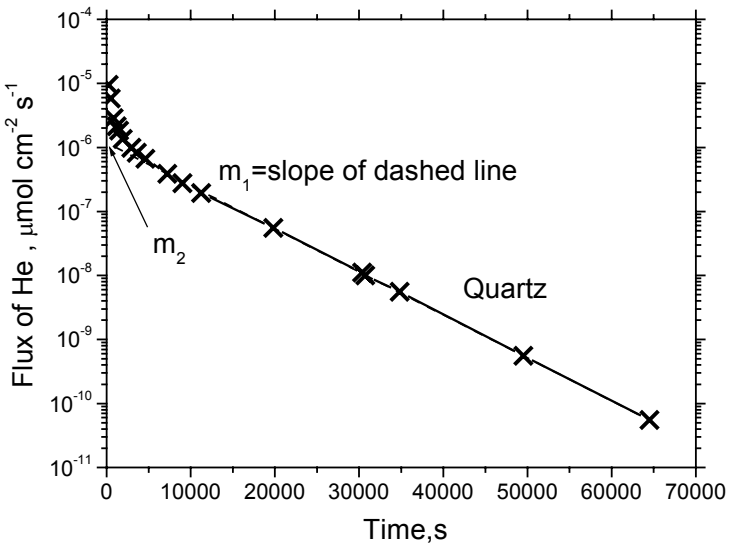

Fig. 4.4 Flux data for He outgassing at 80°C after background subtraction.

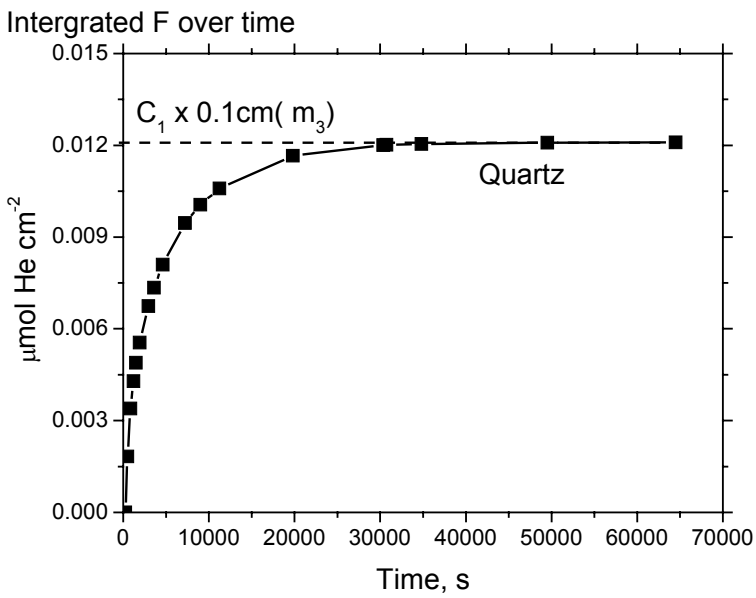

Fig. 4.5 Integrated He flux over time for a vitreous silica plate of thickness 0.1 cm at 80°C.

The diffusivity, concentration and permeability of He in vitreous silica evaluated from this method are in the range with the data from other measurement methods. Therefore, it

indicates that the novel method is valid and can be used to characterize the gas transport in oxides and the results were compared with the existing literature data.

Table 4.1 Transport parameters for He in quartz at 80°C.

Parameters	Our results from this method		Results from references [1, 2]
Diffusivity, $cm^2\ s^{-1}$	D_{m1}	$1.2 \cdot 10^{-7}$	$(1\text{-}2) \cdot 10^{-7}$
	D_{m2}	$1.2 \cdot 10^{-7}$	
Concentration, $\mu mol\ cm^{-3}$	0.12		-
Permeability, $atoms\ s^{-1}\ cm^{-1}\ atm^{-1}$	$3.5 \cdot 10^{10}$		$(4\text{-}6) \cdot 10^{10}$

4.4 The effects of platinum on the oxidation of metals (Papers 1 and 6)

The aim of this study is to identify the overall effect of Pt on the oxidation of metals. Samples of Al, Cr, Ni, and Zr were sputter-coated with porous Pt films with a particle size of 20-30 nm. Thermal oxidation of these samples was studied by gas phase analysis and secondary ion mass spectrometry.

Porous Pt-coatings have two effects on the oxidation of metals. One effect is to enhance the oxide growth at the oxide-metal interface by increasing the inward flux of dissociated oxygen. The other effect is to suppress the oxide growth by reducing the contact area between the substrate and the oxidizing atmosphere.

Platinum is probably the most well known catalytic material for O_2 dissociation. Pt-particles act as generators for dissociated oxygen, which supply a high flux of dissociated oxygen to the metal substrate. For a metal sample coated with an evenly distributed Pt film, Pt effects on oxide growth versus Pt coverage are shown in Fig. 4.6, where Pt dots are assumed to be gas-tight. The O spill over effect increases up to a certain Pt coverage and then decreases due to a competition between the increasing oxygen flux and the decreasing spill over area upon Pt coverage. The Pt suppression effect increases linearly with Pt coverage.

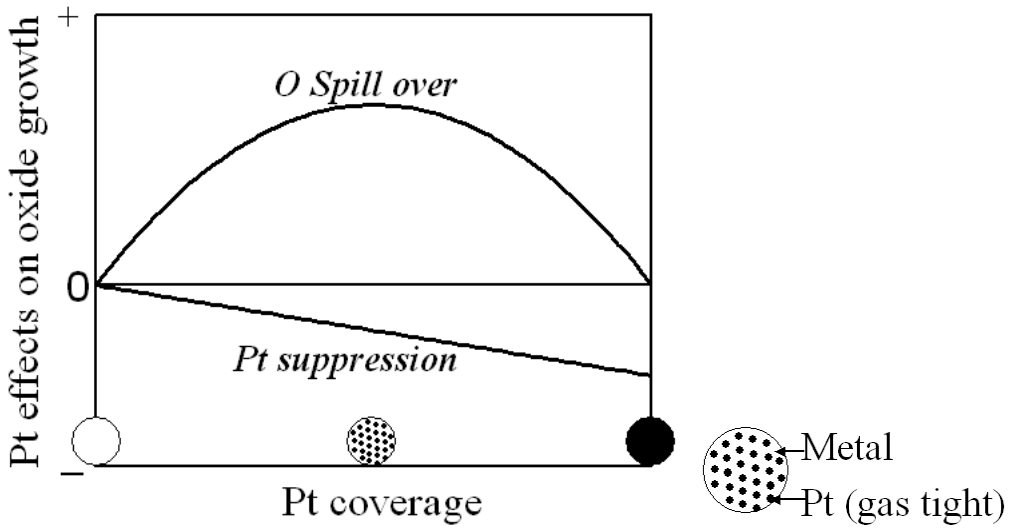

Fig. 4.6 Effects of Pt on the oxidation of a metal vs. Pt coverage (Paper 6).

The effects of Pt on the oxide growth should depend on the mechanisms of oxide growth in the absence of Pt. Formation of oxide on the surface of metals may take place by inward oxygen transport and/or outward metal transport. Fig. 4.7 shows the effects of Pt versus Pt coverage on the oxide growth by exclusive oxygen transport in the absence of Pt. The downward solid arrow denotes inward oxygen flux due to O spill over effect of Pt, O sp, which increases firstly and then decreases upon Pt coverage. The downward dash arrow denotes intrinsic inward oxygen flux after Pt suppression, O in, which decreases linearly with Pt coverage. The overall effect of Pt on the oxide growth of this type of metal, d (O), is proportional to the sum of O sp and O in, d (O) ~ (O sp + O in), as illustrated by the thick solid curve in Fig. 4.7, where d_0 is the oxide growth in the absence of Pt, and d_{max} is the maximal oxide growth. Oxidation of metals is enhanced up to a certain Pt coverage, when the spill over effect is dominant, d (O) > d_0, then oxidation is suppressed when the Pt suppression effect is dominant, d (O) < d_0. For the oxidation of metal samples partly coated with porous Pt films with dominating O transport in the absence of Pt, it leads to a pronounced increased oxide growth taking place on the oxide-metal interface in the Pt-area. It also, to some extent, enhances the oxide growth at a distance from the Pt-area in the adjacent oxide, as schematically shown in Fig. 4.8.

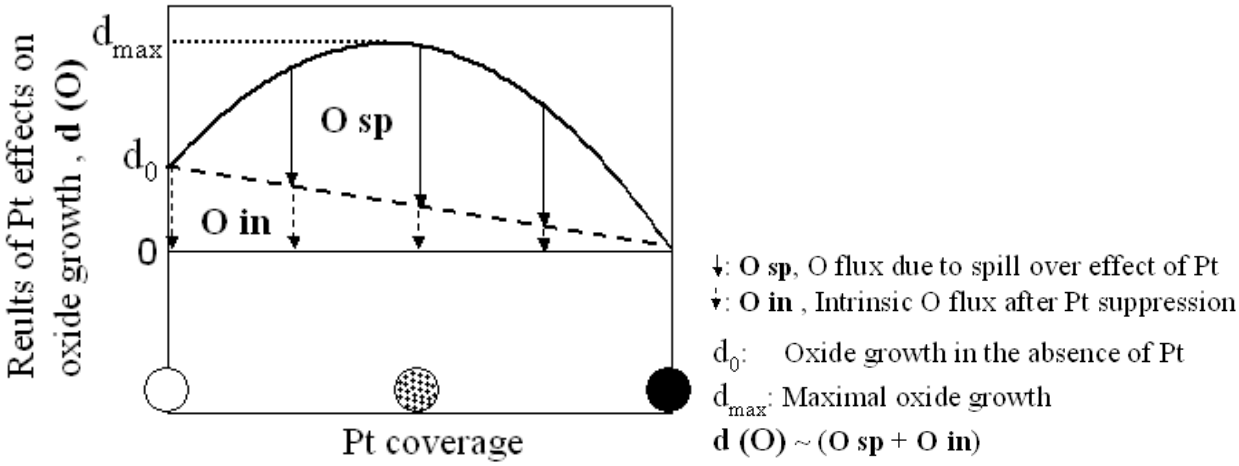

Fig. 4.7 Effects of Pt on the oxidation of a metal with exclusive oxygen transport in the absence of Pt vs. Pt coverage (Paper 6).

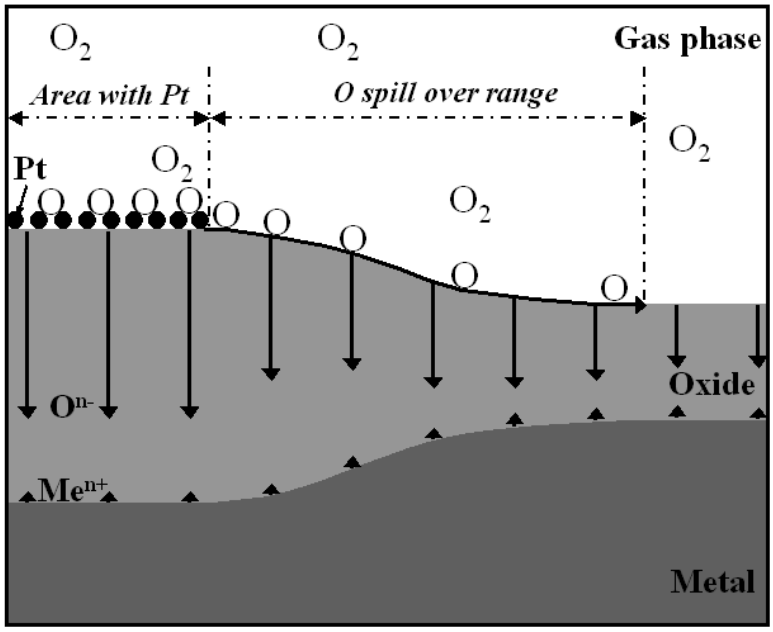

Fig. 4.8 Schematics of the influence of a porous Pt coating on the oxidation of a metal with dominating oxygen transport in the absence of Pt (Paper 6).

Fig. 4.9 shows effects of Pt versus Pt coverage on the oxide growth by exclusive metal transport in the absence of Pt. The downward solid arrow denotes inward oxygen flux due to O spill over effect of Pt, O sp, which increases firstly and then decreases upon Pt coverage. The upward dash arrow denotes intrinsic outward metal flux after Pt suppression, Me in, which decreases linearly with Pt coverage. It is suggested that a balanced oxide growth by stoichiometric oxygen and metal transport results in a formation of protective oxide and a lower oxidation rate. In this case, the dissociated oxygen flux is generated by Pt, which is of benefit for a balanced oxide growth. The overall effect of Pt on the oxidation of this type of metal, d (Me), is estimated by the expression d (Me) ~

(major flux – 0.1 · minor flux), as illustrated with the thick solid curve in Fig. 4.9. In this figure, d_0 is again the oxide growth in the absence of Pt, d_{bal} is the best balanced oxide growth when the oxygen flux equals the stoichimetric metal flux, d_{max} is the maximal oxide growth, major flux is the dominant oxygen or metal flux, and minor flux is non-dominant oxygen or metal flux at the corresponding Pt coverage, 0.1 is a factor of reduced oxidation due to a improved balance and formation of protective oxide which is here estimated by the experimental results of a Ni sample coated with porous Pt presented in Paper 6. The d_{max} in Fig. 4.9 is lower than the d_{max} in Fig. 4.7. The overall effect of Pt firstly reduces the oxide growth due to improved balanced transport, then enhances the oxide growth due to a dominant O spill over effect, afterwards suppresses the oxide growth due to a dominant Pt suppression effect. Fig. 4.10 schematically shows the effects of a porous Pt film on the oxidation of a metal with dominating metal-ion transport in the absence of Pt. In this figure, it is expected a pronounced increase of oxide growth taking place at the oxide-metal interface in the Pt-area and a minimum of oxide growth close to the Pt-area.

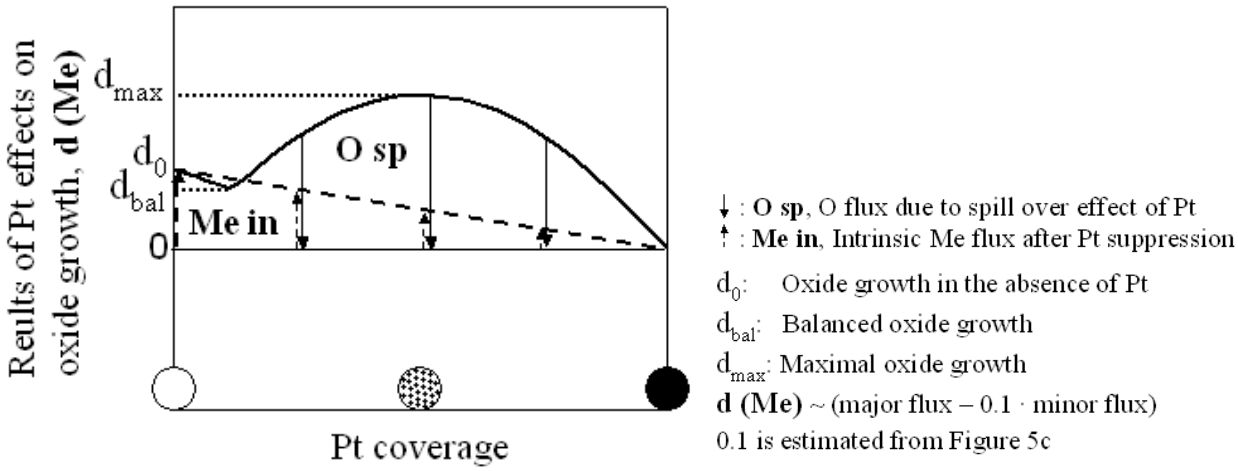

Fig. 4.9 Effects of Pt on the oxidation of a metal with exclusive metal transport in the absence of Pt vs. Pt coverage (Paper 6).

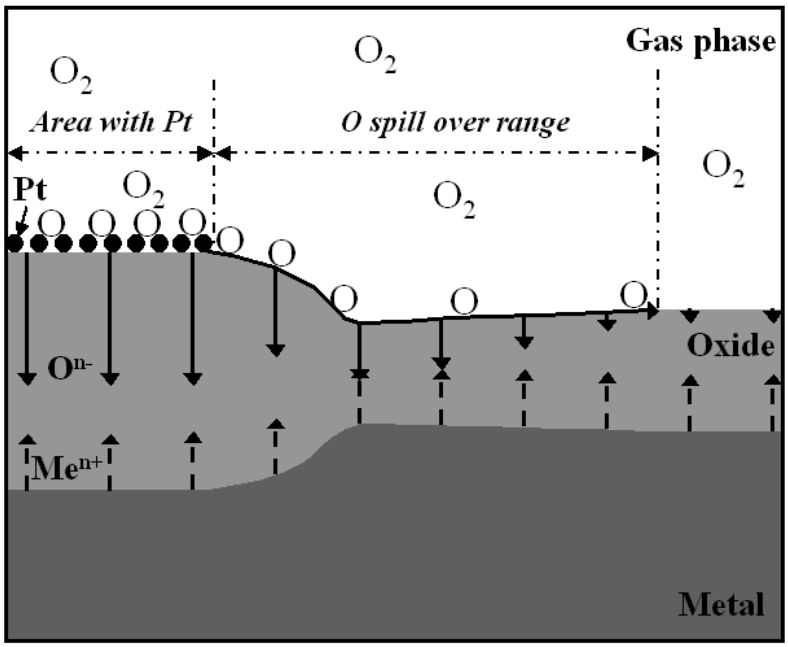

Fig. 4.10 Schematics of the influence of a porous Pt coating on the oxidation of a metal with dominating metal transport in the absence of Pt (Paper 6).

4.5 Transport of diatomic gases in vitreous silica (Papers 2 and 3)

4.5.1 Transport of nitrogen in vitreous silica

Fig. 4.11 summarizes the permeability of the noble gases He, Ne, Ar and Kr and the diatomic gases hydrogen, oxygen and nitrogen in vitreous silica at 900°C. These data are obtained from Refs [1, 3]. The permeability of nitrogen in silica at 900°C is measured to $6 \cdot 10^8$ molecules cm^{-1} s^{-1} atm^{-1} in Paper 3 and is also plotted in Fig. 4.11(▲). It is seen in the figure that the logarithm of the permeabilities vs. molecular collision diameter of the noble gases fall on a straight line, here called the noble gas line.

The diffusion of noble gases in vitreous silica takes place with a single mode diffusion process and the gas has virtually zero chemical interaction with the glass network. Their permeability, or rather diffusivity, is strongly size dependent. The experimentally obtained permeabilities of the diatomic gases, hydrogen, oxygen and nitrogen are significantly higher, 40 times for hydrogen, 35 times for oxygen and 60 times for nitrogen, than expected from values given by the noble gas line, as seen in Fig. 4.11. We consider two possibilities to explain these high permeabilities. One possibility is that a very small fraction (approximately 10^{-4}) of diatomic molecules dissociate and permeate freely in atomic form at a rate determined by a size half that of molecules and on the noble gas line. In a previous study [4] it was found that more than 95% of hydrogen had undergone

dissociation in silica at 900°C, whereas in the present work of nitrogen in Paper 3 the corresponding value is approximately 15%, as seen in Fig. 4.12. We exclude freely permeating atoms primary due to the high degree of dissociation observed compared to 10^{-4}. The second possibility is that several percent of diatomic molecules dissociate into atoms, which are retarded due to an interaction with the host material during diffusion. In effect, this means a reversible trapping of atoms. A retardation of permeating atoms due to reversible trapping should be influenced by the concentration of traps and their interaction strength. In this description, the observed total permeabilities of diatomic gases are the sums of a molecular permeability, roughly indicated by the noble gas line, and a permeability due to reversibly trapped atoms.

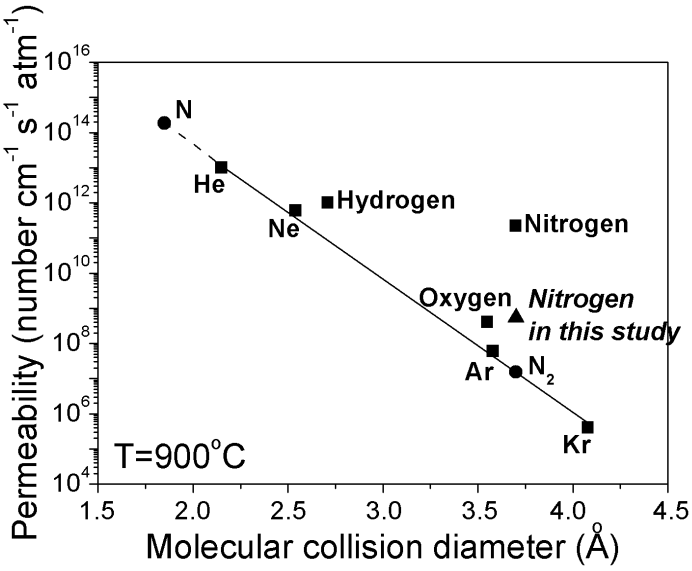

Fig. 4.11 Permeability of noble gases and some diatomic gases in vitreous silica at 900°C from Ref. [1] vs. molecular collision diameter data from Ref. [3] (■). Permeability for nitrogen measured in this study is also plotted in the figure (▲). Permeability of N_2 (●) is determined by the noble gases but found higher in this study. Permeability of N (●) is taken from extrapolation of solid line determined by the noble gases. Diameter of N is assumed to be half that of N_2 (Paper 3).

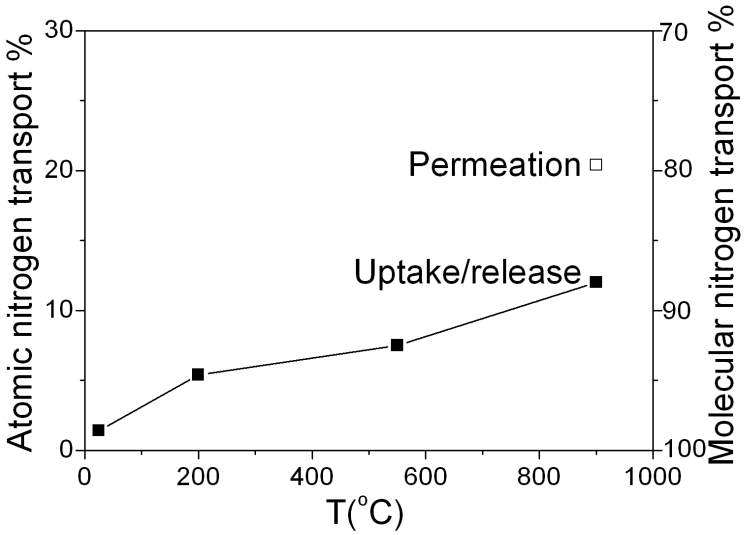

Fig. 4.12 Percentage of atomic and molecular nitrogen transport versus temperature (Paper 3).

4.5.2 Concentration-dependent hydrogen diffusion in vitreous silica related to trapping

The Paper 2 reports experiments on hydrogen permeation through a vitreous silica wall at 550°C with applied hydrogen pressures up to 1200 mbar. For each pressure, and at steady state, the flux and the amount of hydrogen in the material are independently measured. Within the experimental accuracy we find that the flux is proportional to the pressure and that the hydrogen amount increases with a falling gradient with respect to pressure. The result is a relationship between flux and mean concentration. A careful evaluation of the flux versus concentration relationship by means of the steady-state diffusion equation shows that the hydrogen diffusivity in the silica wall is concentration dependent and increases linearly with local concentration. The overall results are shown in Fig. 4.13. Vitreous silica has a disordered structure where hydrogen can be trapped. Shelby reports that the chemical reactions of hydrogen with vitreous silica form hydroxyl and hydride at high temperatures. Hence, there is a finite amount of traps in silica which react with hydrogen. At hydrogen concentrations comparable with the concentration of traps, the transport of hydrogen is suppressed by reversible trapping, while at high hydrogen concentration the transport is less influenced by the finite amount of traps. Reversible trapping explains the observed concentration-dependent diffusivity of hydrogen.

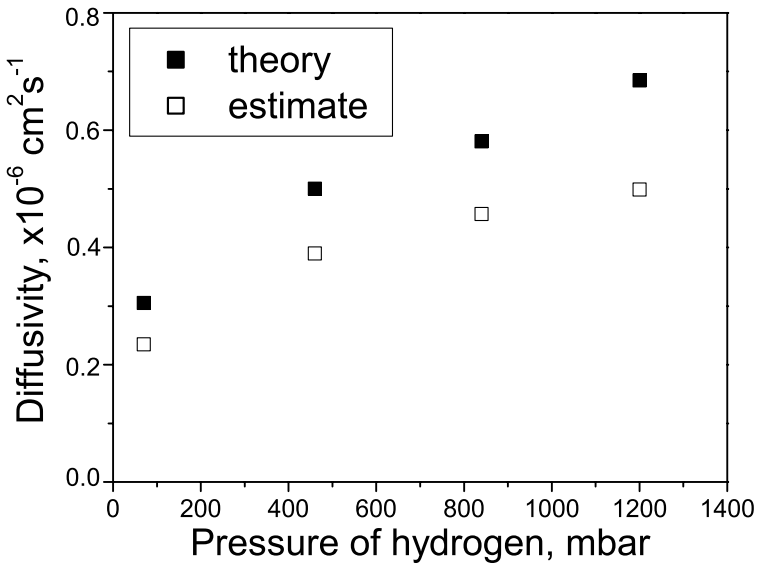

Fig. 4.13 Comparison between theoretical diffusivity and estimated diffusivity of hydrogen in vitreous silica at 550°C corresponding to inlet pressures 70, 460, 840, and 1200 mbar (Paper 2).

4.6 Transport of gases in yttria-stabilized zirconia (Paper 7)

Paper 7 presents the results of permeation experiments of air and a mixture of He + Ar + N_2 + O_2 through a YSZ wall. The results from isotope studies of transported species of diatomic gases H_2, O_2 and N_2 in YSZ are also presented. The aims of this study are to improve the understanding of gas transport properties in YSZ and to offer possible explanations to the observed phenomena.

Theoretical considerations show that the uptake ratio of He/Ar is less than 1.5 in case of no water adsorption and the uptake ratio of He/Ar can exceed 1.5 in case of one monolayer water adsorption on the surface and grain boundaries of yttria stabilized ZrO_2. The experimental uptake ratio of He/Ar at room temperature is in the range of 6 - 10 which indicates that water is adsorbed on the internal and external surfaces.

The percentages of dissociation of diatomic molecules transported in YSZ were estimated according to the principle and analysis method described in Paper 8. The experimental results in Paper 7 show that approximately 7 % of permeated nitrogen has undergone dissociation in YSZ at 950°C, less than 9 % of permeated hydrogen has undergone dissociation in YSZ at 25°C, and approximately 99 % of released oxygen has undergone dissociation in YSZ and mainly in form of oxygen ions at 900°C.

Permeabilities of oxygen and nitrogen upon exposure of YSZ to air and mixed gas were measured at 200 - 980°C. The results are shown in Fig. 4.14, where the permeability of oxygen is higher than that of nitrogen. Permeabilities of oxygen and nitrogen increase

with temperature. Permeability of nitrogen increases relatively smoothly upon increasing temperature, whereas permeability of oxygen upon temperatures shows two zones in both exposure atmospheres. One zone shows a slow increasing permeability at 200 - 800°C; the other zone shows a significant fast increasing permeability at 800-1000°C. These results indicate the diffusion mechanisms of diatomic gases in zirconia may differ upon temperature.

It is found that diatomic gases transport both in molecular and dissociated form in YSZ and the percentage of dissociation of diatomic molecules transported in YSZ depends on the temperature and properties of gases. A two-zone curve is expected in Fig. 4.14 due to a higher percentage of dissociation of diatomic molecules at higher temperature and a higher permeability of dissociated species.

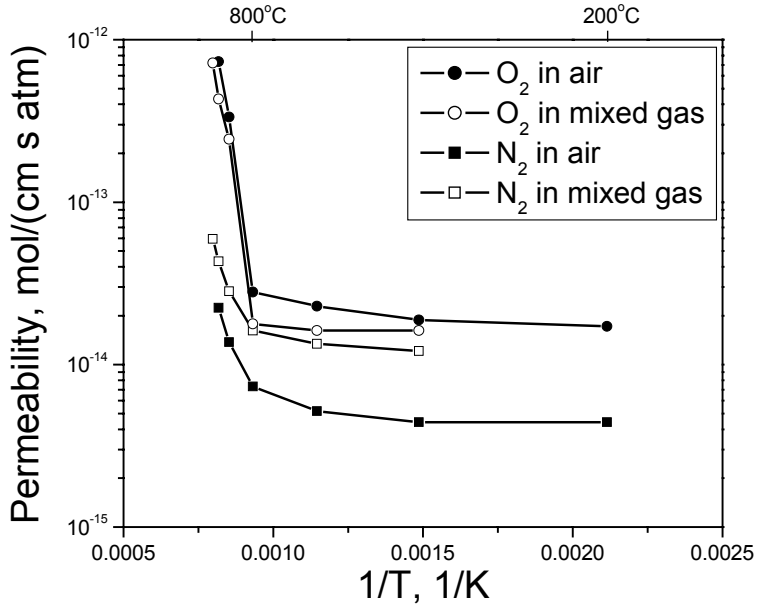

Fig. 4.14 Permeabilities of oxygen and nitrogen vs. reciprocal temperature upon exposure of YSZ to air and mixed gas.

Transport paths are shared among transported species and gases at all temperatures in YSZ. He shares transport path with molecular oxygen and nitrogen at low temperatures (Fig. 4.15), whereas He shares transport path with dissociated oxygen and also dissociated nitrogen, respectively, at high temperatures due to the relative small size of He (Fig. 4.16).

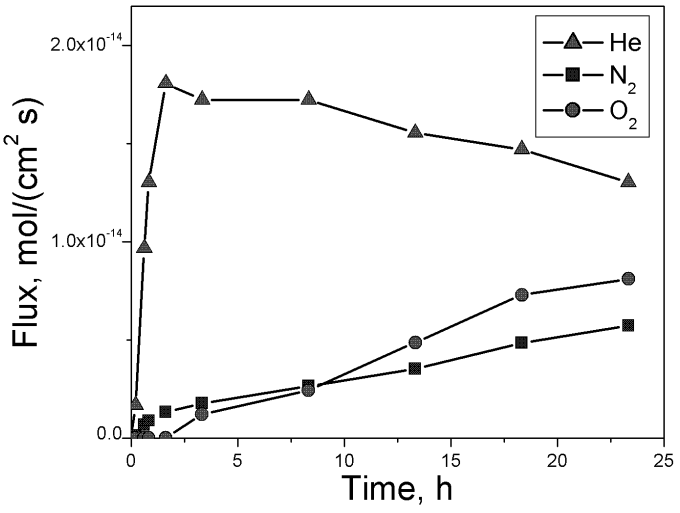

Fig. 4.15 Transient flux of helium, oxygen, and nitrogen through a 2 mm thick YSZ wall upon exposure to 1000 mbar mixed gas at 200°C.

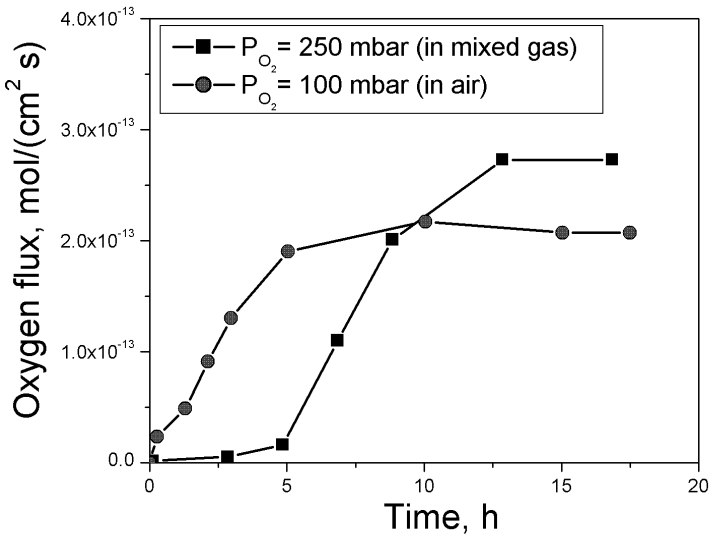

Fig. 4.16 Comparison of transient oxygen flux through a 2 mm thick YSZ wall upon exposure to mixed gas and air when temperature increases from 800 °C to 900°C.

References

1. J. E. Shelby, Handbook of Gas Diffusion in Solids and Melts, ASM Interntaional, 1996
2. D. E. Swets, R. W. Lee, R. C. Frank, J. Chem. Phys., 34 (1961), 17
3. D. R. Lide, CRC Handbook of Chemistry and Physics, 80th ed. CRC Boca Raton, 1999
5. E. Hörnlund and G. Hultquist, J. Appl. Phys., 94 (2003), 4819

Chapter 5

Concluding remarks

Transport in oxides is studied by using the gas phase analysis technique in this thesis. The results from the study contribute the knowledge mainly in the following three areas:

1. An experimental method to identifying transporting species of gases and their contribution to the overall transport of gases in oxides and an experimental method to evaluate the transport related parameters such as diffusivity, concentration, permeability of gases in oxides, and effective pore size in oxides are developed by the use of gas phase analysis.

2. Studies of the influence of porous Pt coating on the thermal oxidation of metals show that:

- Pt acts as a generator for dissociated oxygen and a mm-ranged influence of Pt is frequently observed, which can be explained by a fast surface diffusion of dissociated oxygen on the external surface of the oxide.
- A primary effect of Pt-coating is to promote an increased concentration gradient of dissociated oxygen across the oxide scale, which results in an increased inwards transport of dissociated oxygen and an enhanced oxide growth near the metal substrate. Pt also has a suppression effect on the metal oxidation due to a lower contact area between metal and oxygen. The overall effect of Pt on the oxidation of metals depends on mechanisms of oxide growth in the absence of Pt.
- It is suggested that an appropriate amount of Pt coating induces a balanced oxide growth resulting from stoichimetric inward oxygen flux to outward metal flux, which leads to a reduced oxidation rate.

3. Studies of the transport of gases in vitreous silica and yttria stabilized zirconia (YSZ) show that:

- The diffusion of diatomic gases in oxides takes place in both molecular and dissociated (atomic or /and ionic) form. The fraction of transport of molecular

species decreases with the temperature, and that of transport of dissociated species increases with the temperature.

- Measured permeabilities of hydrogen, oxygen, and nitrogen in vitreous silica are higher than the expected permeabilities of their molecules. The observed total permeabilities of diatomic gases in vitreous silica are explained by the sum of a molecular permeability and permeability of reversibly trapped atoms.
- A concentration – dependent diffusion of hydrogen in vitreous silica at 550°C is explained by an effective diffusivity due to a finite amount of reversible traps of hydrogen in the material.
- Transport paths are shared among transported species and gases at all temperatures in YSZ. Helium shares transport path with molecular oxygen and nitrogen at low temperatures; whereas helium shares transport path with dissociated oxygen and also dissociated nitrogen at high temperatures.

Chapter 6

Outlook

Some suggestions of investigation that may be interesting to carry out in the future are listed below:

In the thesis, the effects of Pt on oxidation of metals have been studied. The effects of Pt on the oxidation of alloys such as NiAl and FeCrSi have already been started in the similar way but need further investigations by SIMS analysis and comparisons are needed in order to obtain a wider perspective. It may lead to development of new application in the formation of protective metal-oxides.

It is found that the hydrogen concentration at steady state in vitreous silica is not linearly pressure-dependent. Together with concentration dependent hydrogen diffusivity in vitreous silica, it should be pointed out that the linear pressure dependence of flux found in Paper 2 is rather a coincidence than a fundamental relation. The finding deserves further examination in other systems so as to verify the findings.

Transport studies of hydrogen, oxygen, and nitrogen in alumina and chromia would be interesting to perform. The comparison of transport properties in different oxides will be helpful to fundamentally understand the importance in high temperature corrosion.

Chapter 7

Acknowledgments

I would like to take this opportunity to express my gratitude and appreciation to the following people who have contributed in different ways towards the completion of this thesis:

Doc. G. Hultquist, my supervisor, for his inspiring guidance, his endless enthusiasms to discuss the academic topics, clarifying my thinking, helping me to define the correct questions. Especially, I appreciate his prompt response to my numerous manuscripts even in difficult period. Without his help, the thesis can not be completed.
All my present and former colleagues at the Division of Corrosion Science for providing a friendly working atmosphere. Especially I would like to thank Prof. C. Leygraf for creating the chance to undertake this study, Doc. J. Pan and Dr. W. He for their great help when I just arrived at Sweden and sharing their experience and knowledge through years, Dr. P. Szakalos for his help on microscopy and good comments on my work, and Doc. I. O. Wallinder for her kind help with many routine matters. It has been a pleasure working with all of you.
Dr. J. Rundgren at Department of Theoretical Physics at KTH for many fruitful discussions and valuable ideas and Dr. M. Graham at National Research Council of Canada for his cooperation and showing interests in my work.
Prof. S. Baldelli at University of Houston for his sincere concerns and encouragements.
My entire family in China and Sweden, which is the harbor of my heart forever. Especially, My husband, Yanbing, I appreciate his continuous and solid support in many aspects. My parents in law for their help to take care of our baby in the first year when I was back to work from parental leave. My lovely son, Yingnan, for his angel-like laughs and joyful time we have spent together which always give me the most relaxation.

Finally, financial support from Swedish Foundation for Strategic Research is gratefully acknowledged. Also some support from the Swedish Competence Center for High Temperature Corrosion should be mentioned.

Qian Dong (董倩)

Stockholm, April 2007